

1 The first *de novo* HiFi genome assemblies for three clownfish-hosting sea anemone
2 species (Anthozoa: Actiniaria)

3

4 Aurélien De Jode^{*1,2}, Benjamin M. Titus^{1,2}

5

6 ¹Department of Biological Sciences, University of Alabama, Tuscaloosa, AL, USA.

7 ²Dauphin Island Sea Lab, Dauphin Island, AL, USA.

8

9 *Author for Correspondence: Aurélien De Jode, Department of Biological Sciences,
10 University of Alabama, Tuscaloosa, AL, USA, aurelien.dejode@laposte.net

11

12

13

14

15

16

17

18

19

20

21

22

23

24

25

26 **Abstract**

27 The symbiosis between clownfish and giant tropical sea anemones (Order Actiniaria) is one of
28 the most iconic on the planet. Distributed on tropical reefs, 28 species of clownfishes form
29 obligate mutualistic relationships with 10 nominal species of venomous sea anemones. Our
30 understanding of the symbiosis is limited by the fact that most research has been focused on
31 the clownfishes. Chromosome scale reference genomes are available for all clownfish species,
32 yet there are no published reference genomes for the host sea anemones. Recent studies have
33 shown that the clownfish-hosting sea anemones belong to three distinct clades of sea
34 anemones that have evolved symbiosis with clownfishes independently. Here we present the
35 first high quality long read assemblies for three species of clownfish hosting sea anemones
36 belonging to each of these clades: *Entacmaea quadricolor*, *Stichodactyla haddoni*,
37 *Radianthus doreensis*. PacBio HiFi sequencing yielded 1,597,562, 3,101,773, and 1,918,148
38 million reads for *E. quadricolor*, *S. haddoni*, and *R. doreensis*, respectively. All three
39 assemblies were highly contiguous and complete with N50 values above 4Mb and BUSCO
40 completeness above 95% on the Metazoa dataset. Genome structural annotation with
41 BRAKER3 predicted 20,454, 18,948 and 17,056 protein coding genes in *E. quadricolor*, *S.*
42 *haddoni* and *R. doreensis* genome, respectively. These new resources will form the basis of
43 comparative genomic analyses that will allow us to deepen our understanding of this
44 mutualism from the host perspective.

45

46 **Keywords:** Cnidaria, Actinoidea, Symbiosis

47 **Significance**

48 Chromosome-scale genomes are available for all 28 clownfish species yet there are no high-
49 quality reference genomes published for the clownfish-hosting sea anemones. The lack of
50 genomic resources impedes our ability to understand evolution of this iconic symbiosis from
51 the host perspective. The clownfish-hosting sea anemones belong to three clades of sea
52 anemones that have evolved mutualism with clownfish independently. Here we assembled the
53 first high-quality long-read genomes for three species of host sea anemones each belonging to
54 a different host clade: *Entacmaea quadricolor*, *Stichodactyla haddoni*, *Radianthus doreensis*.
55 These resources will enable in depth comparative genomics of clownfish-hosting sea
56 anemones providing a critical perspective for understanding how the symbiosis has evolved.
57 Finally, these reference genomes present a significant increase in the number of high-quality
58 long-read genome assemblies for sea anemones (11 currently published) and double the
59 number of high-quality reference genomes for the sea anemone superfamily Actinoidea.

60 **Introduction**

61 Among all mutualistic symbioses none are more recognizable than the association
62 between clownfishes (also called anemonefishes: Subfamily Amphiprioninae) and their giant
63 host sea anemones (Anthozoa: Actiniaria). Distributed broadly on tropical coral reefs
64 throughout the Indian and Pacific Oceans, 28 species of clownfishes have rapidly radiated to
65 form obligate mutualistic relationships with 10 nominal species of venomous sea anemones
66 (Litsios et al., 2012; Gaboriou et al., 2024; Titus et al. 2024). Famously, clownfishes have
67 evolved to live unharmed in their toxic and venomous hosts benefiting from their association
68 with sea anemones by receiving shelter against predators (Fautin 1991), protection for their
69 externally brooded eggs (Fautin & Allen 1992), removal of external parasites (Lubbock 1981)
70 and potentially even nourishment (Verde et al., 2015). In turn, sea anemones are granted
71 reciprocal protection against predation (Dunn 1981, Godwin & Fautin, 1992, Holbrook &
72 Schmitt, 2005), novel sources of nitrogen and carbon from fish excrement (Roopin et al.
73 2008, Roopin & Chadwick, 2009, Cleveland et al., 2011), and increased oxygenation and gas
74 transfer as clownfishes move through their tentacles (Szczebak et al. 2013).

75 The symbiosis has attracted a great deal of popular and scientific attention. The
76 small size of clownfishes and their well-defined hierarchical social groups, reproductive
77 biology, and amenability to aquaculture have made them tractable systems for understanding
78 fundamental biological processes. They are now considered an emerging model organism for
79 a wide range of research (Roux et al., 2020; Laudet & Ravasi, 2022). Chromosome-level
80 reference genomes are now available for all 28 clownfish species (Marcionetti et al., 2019;
81 Marcionetti & Salamin, 2023; Gaboriou et al., 2024) and comparative analyses are revealing
82 the first candidate genes likely to be associated with the ability of clownfishes to remain

83 protected from toxic sea anemone hosts (Marcionetti et al., 2019; Marcionetti & Salamin,
84 2023).

85 Our evolutionary understanding of the symbiosis, however, is limited by the fact
86 that most research and genomic resources have been focused on clownfishes. No reference
87 genomes exist for any of the 10 clownfish-hosting sea anemones. This perspective is expected
88 to be especially critical as recent work has demonstrated that the host sea anemones are
89 driving phenotypic convergence in clownfishes (Gaboriau et al., 2024), and that host sea
90 anemones have diversification times that are broadly concomitant with the clownfish radiation
91 (De Jode et al. 2024). These findings highlight the importance of the host sea anemones for a
92 holistic understanding of the entire symbiosis. High-quality reference genomes for the host
93 sea anemones thus hold the potential to identify genomic regions associated with establishing
94 and maintaining mutualism with clownfishes, and other genomic consequences of a symbiotic
95 lifestyle.

96 Interestingly, unlike the 28 described species of clownfishes which form a
97 monophyletic clade, the 10 clownfish hosting sea anemones belong to three distinct lineages
98 within the sea anemone superfamily Actinoidea that have evolved symbiosis with
99 clownfishes (Titus et al. 2019; 2024; De Jode et al. 2024). These have been coined
100 *Entacmaea*, Stichodactylina, and Heteractina. The clade *Entacmaea* contains only the bubble-
101 tip sea anemone, *Entacmaea quadricolor* (Fig. 1A), which appears to be a species complex
102 (Titus et al. 2019; De Jode et al. 2024). Clade Stichodactylina contains five clownfish hosting
103 sea anemones species: *Cryptodendrum adhaesivum*, *Radianthus magnifica*, *Stichodactyla*
104 *gigantea*, *S. haddoni* (Fig. 1B), and *S. mertensii*, as well as other non-host species (e.g. De
105 Jode et al. 2024). Clade Heteractina includes *Heteractis aurora*, *Radianthus crispa*, *R.*
106 *doreensis* (Fig. 1C), and *R. malu* (Titus et al. 2019; De Jode et al. 2024). The three

107 independent clades of host sea anemones provide a natural starting point for sequencing and
108 assembling high-quality reference genomes.

109 Here we present the first high quality long reads assemblies for three species of
110 clownfish hosting sea anemones: *Entacmaea quadricolor*, *Stichodactyla haddoni*, and
111 *Radianthus doreensis* (Fig. 1). These genomes will form the basis for in depth comparative
112 genomics between clownfish hosting and non-hosting sea anemones and deepen our
113 understanding of this iconic symbiosis.

114

115 **Results and Discussion**

116 A total of 1,597,562 (~ 20 Gbp), 3,101,773 (~ 39 Gbp) and 1,918,148 (~26 Gbp)
117 HiFi reads were sequenced for *E. quadricolor*, *S. haddoni* and *R. doreensis*, respectively.
118 For each species, mitochondrial genomes were assembled, circularized, and annotated. The
119 total lengths of the newly assembled mitochondrial genomes were 20,761 bp, 18,921 bp, and
120 19,768 bp for *E. quadricolor*, *S. haddoni* and *R. doreensis* (Fig. 1), respectively. These are
121 similar to the size of the mitogenomes used as references to identify mitochondrial reads. A
122 characteristic feature of Hexacorallian mitogenomes is the presence of a self-splicing intron in
123 the NAD5 gene (Feng et al., 2023). Interestingly, MitoFinder (the default annotation tool of
124 MitoHiFi) did not retrieve that feature in our mitogenomes, but we were able identify and
125 retrieve the NAD5 intron using MITOS in all species. Feng et al. (2023) identified a
126 conserved mitochondrial gene order in the Order Actiniaria. Using the annotation conducted
127 in GeSeq we confirmed that our three mitogenomes shared that same order (Act1GO sensu
128 Feng et al. 2023).

129 Nuclear genome size estimates from GenomeScope were comparable between *S.*
130 *haddoni* (339 Mbp) and *R. doreensis* (330 Mbp). The assembled genomes of *S. haddoni* and
131 *R. doreensis* spanned 447 Mb and 418 Mb, respectively (supplementary table S1), both

132 exceeding GenomeScope estimates by approximately 100 Mb. *Entacmaea quadricolor* had
133 the largest estimated genome size at 578 Mbp, which was close to our final total assembly
134 length of 599 Mb (supplementary table S1). Our genome size estimate for *E. quadricolor* was
135 smaller than the 863 Mbp estimated using flow cytometry (Adachi et al., 2017), but higher
136 than the 428 Mb assembly available on GenBank (GCA_024752375.1). The discrepancy
137 between our PacBio assembly and the publicly available assembly is likely due to the latter
138 genome being assembled using Illumina short reads.

139 Heterozygosity rates were comparable between *R. doreensis* (het: 0.767%) and *S.*
140 *haddoni* (het: 0.855%) but were higher in *E. quadricolor* (het: 1.49 %). Merqury k-mer
141 spectra plots revealed the presence of haplotypic duplications in each primary assembly
142 (supplementary fig. 1). For each species, the assembly we obtained after using the purge_dups
143 algorithm with manual cutoffs and contigs identified as repeats added back into the assembly,
144 showed the best compromise between under and over purging and was kept for further
145 analysis (supplementary fig. 1). A total of 17, 8 and 8 contigs were identified as contaminants
146 and removed from the *E. quadricolor*, *S. haddoni* and *M. doreensis* assemblies, respectively
147 (supplementary fig. 2). One mitochondrial contig was also identified and removed from each
148 assembly.

149 Final genome assemblies were highly contiguous and comprised of 558, 648 and
150 230 contigs for *E. quadricolor*, *S. haddoni* and *R. doreensis*, respectively. N50 values were
151 roughly 4 Mb (*E. quadricolor*), 5.3 Mb (*S. haddoni*), and 8 Mb (*R. doreensis*) (supplementary
152 table 1). BUSCO completeness scores for the Metazoa dataset were 95.6 % for *E. quadricolor*
153 and *S. haddoni* and 95.4 % for *R. doreensis* (supplementary table 1). A total of 20,454,
154 18,948 and 17,056 protein coding genes were predicted by the BRAKER3 annotation pipeline
155 for *E. quadricolor*, *S. haddoni* and *R. doreensis* respectively (Fig. 2). For each species the

156 total number of predicted proteins were comparable to the number of predicted proteins for
157 other members of Order Actiniaria (Fig. 2).

158 The OMArk completeness percentages, based on Hierarchical Orthologous Groups
159 (HOGs) of genes in Eumetazoa, were 92.6%, 92.35 % and 85.53 % for *E. quadricolor*, *S.*
160 *haddoni* and *R. doreensis*, respectively (Fig. 2, supplementary text). The OMArk consistency
161 assessment was very similar among our three species and other members of Order Actiniaria
162 (Fig. 2, supplementary text). OMArk consistency (the gene family is known to exist in the
163 Eumetazoa lineage) scores 70.16 %, 72.27 % and 71. 56 % for *E. quadricolor*, *S. haddoni* and
164 *R. doreensis*, respectively. No protein sequence was identified as a contaminant in any of our
165 species. The lower amount of protein coding genes predicted in *S. haddoni* and *R. doreensis*
166 and the lower level of completeness in *R. doreensis* are likely due to the lower amount of
167 RNA seq data available for those species (supplementary text). The ratio of mono- to multi-
168 exonic transcripts were 0.34, 0.28 and 0.34 for *E. quadricolor*, *S. haddoni* and *R. doreensis*
169 respectively.

170

171 **Conclusion**

172 Prior to this study, no genomes had been published for the clownfish-hosting sea anemones,
173 although chromosome level genomes are available for all 28 species of clownfishes (Gaboriau
174 et al. 2024). The three high-quality genomes we've assembled here using PacBio HiFi reads
175 belong to species from the three clades that have independently evolved mutualism with
176 clownfishes (Titus et al., 2019; De Jode et al., 2024). These will thus become critical new
177 resources for comparative genomics and our understanding of clownfish-hosting sea
178 anemones diversification and of the evolution of the iconic mutualism. Finally, only 11 long-
179 read genomes have been assembled and published for Order Actiniaria. Our genomes

180 represent a significant increase in the number of genomic resources available for
181 understanding sea anemone biology and evolution broadly.

182

183 **Material and Methods**

184 Live sea anemones were purchased via the ornamental aquarium trade through
185 Quality Marine Inc. to ensure the geographic origin of each animal. We acquired three
186 species: the bubble tip sea anemone *Entacmaea quadricolor* (Fiji), Haddon's carpet sea
187 anemone *Stichodactyla haddoni* (Vietnam), and the long-tentacled sea anemone *Radianthus*
188 *doreensis* (Vietnam). Fresh or flash frozen pedal disc tissue was thinly sliced from each
189 anemone to avoid endosymbiotic dinoflagellate contamination and used for DNA extractions.
190 High Molecular Weight (HMW) DNA was extracted using PacBio Nanobind® tissue kits
191 following manufacturer instructions with the exception that the quantity of proteinase K was
192 increased to 40µL. DNA samples were purified with Monarch Nucleic Acid Purification Kit
193 (New England BioLabs, Ipswich, Massachusetts) prior to shearing on a Megaruptor 2
194 (Diagenode, Denville, NJ), at 20kb setting.

195 Libraries were constructed and sequenced at Maryland Genomics at the Institute for
196 Genome Sciences, University of Maryland School of Medicine. Samples were prepared using
197 SMRTbell Prep Kit 3.0 (Pacific Biosciences, Menlo Park, CA) with barcoded adaptors, and
198 subsequently size-selected on BluePippin instrument (Sage Science, Beverly, MA) to remove
199 DNA fragments less than 10kb in size, followed by an equimolar pooling. The pooled
200 libraries were bound to Revio polymerase, then sequenced with a Revio Sequencing Plate and
201 flow cell on a PacBio Revio platform (Pacific Biosciences, Menlo Park, CA). Mitochondrial
202 genomes were assembled from raw HiFi reads using the MitoHiFi v2. (Uliano-Silva et al.,
203 2023) pipeline with default parameters except for the –max-read-len option that was set to 2.
204 Mitochondrial reads were identified for *E. quadricolor*, *S. haddoni*, and *R. doreensis* using the

205 mitogenomes of *E. quadricolor* (Genbank NC_049066.1); *Heteractis aurora* (Genbank
206 NC_047219.1) and *S. haddoni* (MW760873.1, Johansen et al., 2021), respectively.
207 Mitochondrial genome annotation was performed using both MitoFinder (Allio et al., 2020)
208 and MITOS (Bernt et al., 2013). A final annotation was conducted using GeSeq (Tillich et al.,
209 2017) (see explanations in Results & Discussion section). Mitogenomes were visualized using
210 Geneious version 2024.0 (<https://www.geneious.com>) created by Biomatters.

211 Genome sizes and heterozygosities were estimated using GenomeScope 2.0
212 (Ranallo-Benavidez et al., 2020) based of k-mer histogram frequencies generated by Jellyfish
213 v2.3.0 (Marçais & Kingsford, 2011) for a k-mer size of 21bp (Vulture et al. 2017). Nuclear
214 genomes were assembled using Hifiasm v0.19.8-r603 (Cheng et al., 2021) and the first set of
215 partially phased contigs was used for the following analysis.

216 Haplotypic duplications, were removed from the assemblies using the purge_dups
217 v1.2.5 (Guan et al., 2020) algorithm with the following customs cutoffs: (3, 18, 18, 19, 19,
218 180), (20, 54, 54, 55, 55, 240) and (7, 39, 39, 40, 40, 200) for *E. quadricolor*, *S. haddoni* and
219 *M. doreensis*, respectively. Contigs classified as repeats by purge_dups were added back to
220 the assemblies. The Blob toolkit (Laetsch & Blaxter, 2017, Challis et al. 2020) v3.4.3 pipeline
221 was then used to assess the presence of contaminant contigs in each assembly. Mitochondrial
222 contigs were removed from decontaminated nuclear contigs using MitoHiFi v2. (Uliano-Silva
223 et al., 2023) with the mitochondrial genome assembled from the reads as a reference.

224 Genomes were annotated using the BRAKER3 pipeline v.3.0.8 (Gabriel et al. 2024)
225 specifying a BUSCO lineage (--busco_lineage=metazoa_odb10). The pipeline uses several
226 sub-pipelines and third-party tools (Stanke et al., 2006, Gotoh, 2008, Stanke et al., 2008,
227 Iwata & Gotoh, 2012, Simão et al., 2015, Buchfink et al., 2015, Hoff et al., 2016, Hoff et al.,
228 2019, Kovaka et al., 2019, Pertea & Pertea, 2020, Brůna et al., 2021, Gabriel et al., 2021,
229 Huang & Li, 2023, Li, 2023, Brůna et al., 2024) to predict highly reliable genes in reference

230 genome using protein and RNA-seq data. RNA-seq data (see SI for list of accession numbers)
231 were downloaded from Genbank using the fastq-dump function of the SRA-toolkit v.3.0.7
232 (SRA Toolkit Development Team) and reads were mapped to the genome using HISAT2
233 v.2.2.1 (Kim et al. 2019) with the --dta option. The Metazoa partition of the OrthoDB v11
234 protein database was used as evidence for BRAKER 3 (Kuznetsov et al., 2023). To compute
235 the ratio of mono- to multi-exon genes we used the analyze_exons.py script from the GALBA
236 github repository (<https://github.com/Gaius-Augustus/GALBA>). Annotation quality was
237 assessed with use OMArk v.0.3.0 (Nevers et al., 2022) on the OMArk public webserver
238 (<https://omark.omabrowser.org/home/>). Genome quality was assessed for the final assembly
239 and at several intermediate steps during the assembly process. Contiguity and completeness
240 metrics were computed using gfastats v1.3.6 (Formenti et al., 2022) and BUSCO v5.6.1
241 (Manni et al. 2021). Completeness, quality and levels of haplotypic duplication were assessed
242 using Merqury (Rhie et al. 2020) based on HiFi reads.

243

244 **Acknowledgments**

245 We thank members of the Titus Lab for help with sample processing and Rebecca Varney for
246 advice on high molecular weight DNA extractions. We thank Maryland Genomics at the
247 Institute for Genome Sciences, University of Maryland School of Medicine for library
248 preparation and sequencing. We also thank Giulio Formenti and Jonathan M. Wood for
249 helpful discussion regarding the purging of haplotypic duplications. Funding for this work
250 was provided by the University of Alabama and National Science Foundation Grant DEB-
251 1934274 to BMT.

252

253 **Data Availability**

254 The HiFi PacBio sequencing reads, are deposited in NCBI under the BioProject accession
255 numbers PRJNA1076568. The final genome assembly and genome annotation will be
256 deposited under the same BioProject upon publication.

257

258 **Literature Cited**

259

260 Adachi, K., Miyake, H., Kuramochi, T., Mizusawa, K., & Okumura, S. 2017. Genome size
261 distribution in phylum Cnidaria. *Fisheries Science*, 83(1), 107–112.
262 <https://doi.org/10.1007/s12562-016-1050-4>

263

264 Allio, R., Schomaker-Bastos, A., Romiguier, J., Prosdocimi, F., Nabholz, B., & Delsuc, F.
265 2020. MitoFinder: Efficient automated large-scale extraction of mitogenomic data in target
266 enrichment phylogenomics. *Molecular Ecology Resources*, 20(4), 892–905.
267 <https://doi.org/10.1111/1755-0998.13160>

268

269 Bernt, M., Donath, A., Jühling, F., Externbrink, F., Florentz, C., Fritzsch, G., Pütz, J.,
270 Middendorf, M., & Stadler, P. F. 2013. MITOS: Improved *de novo* metazoan mitochondrial
271 genome annotation. *Molecular Phylogenetics and Evolution*, 69(2), 313–319.
272 <https://doi.org/10.1016/j.ympev.2012.08.023>

273

274 Brúna T, Hoff KJ, Lomsadze A, Stanke M, Borodovsky M. 2021. BRAKER2: Automatic
275 Eukaryotic Genome Annotation with GeneMark-EP+ and AUGUSTUS Supported by a
276 Protein Database. *NAR Genomics and Bioinformatics*. 3(1), lqaa108.
277

278 Brúna, T., Lomsadze, A., & Borodovsky, M. 2024. GeneMark-ETP significantly improves the
279 accuracy of automatic annotation of large eukaryotic genomes. *Genome Research*, 34(5),
280 757–768. <https://doi.org/10.1101/gr.278373.123>

281

282 Buchfink B, Xie C, Huson DH. 2015. Fast and sensitive protein alignment using DIAMOND.
283 *Nature Methods*. 12(1), 59-60.

284

285 Challis R, Richards E, Rajan J, Cochrane G, Blaxter M. 2020. BlobToolKit – Interactive
286 Quality Assessment of Genome Assemblies. *G3* (Bethesda) 10:1361–1374. doi:
287 [10.1534/g3.119.400908](https://doi.org/10.1534/g3.119.400908).

288

289 Cleveland, A., Verde, E.A. and Lee, R.W., 2011. Nutritional exchange in a tropical tripartite
290 symbiosis: direct evidence for the transfer of nutrients from anemonefish to host anemone and
291 zooxanthellae. *Marine Biology*, 158, pp.589-602.

292

293 De Jode, A., Quattrini, A. M., Chiodo, T., Daly, M., McFadden, C. S., Berumen, M. L.,
294 Meyer, C. P., Mills, S., Beldade, R., Bartholomew, A., Scott, A., Reimer, J. D., Yanagi, K.,
295 Fuji, T., Rodríguez, E., & Titus, B. M. 2024. Phylogenomics reveals coincident divergence
296 between giant host sea anemones and the clownfish adaptive radiation. *bioRxiv*,
297 2024.01.24.576469. <https://doi.org/10.1101/2024.01.24.576469>

298

299 Dunn, D.F., 1981. The clownfish sea anemones: Stichodactylidae (Coelenterata: Actiniaria)
300 and other sea anemones symbiotic with pomacentrid fishes. *Transactions of the American
301 Philosophical Society*, 71(1), pp.3-115.

302

303 Fautin, D.G., 1991. Review article The Anemonefish Symbiosis: What is Known and What is
304 Not. *Symbiosis*.

305

306 Feng, H., Lv, S., Li, R., Shi, J., Wang, J., & Cao, P. 2023. Mitochondrial genome comparison
307 reveals the evolution of cnidarians. *Ecology and Evolution*, 13(6), e10157.
308 <https://doi.org/10.1002/ece3.10157>

309

310 Formenti G, et al. 2022. Merfin: improved variant filtering, assembly evaluation and polishing
311 via k-mer validation. *Nature Methods*.19:696–704. doi: [10.1038/s41592-022-01445-y](https://doi.org/10.1038/s41592-022-01445-y).

312

313 Formenti G, et al. 2022. Gfastats: conversion, evaluation and manipulation of genome
314 sequences using assembly graphs. *Bioinformatics* 38:4214–4216. doi:
315 [10.1093/bioinformatics/btac460](https://doi.org/10.1093/bioinformatics/btac460).

316

317 Gaboriau, T., Marcionetti, A., Garcia Jimenez, A., Schmid, S., Fitzgerald, L.M., Micheli, B.,
318 Titus, B. and Salamin, N. 2024. Host-use drives convergent evolution in clownfish and
319 disentangles the mystery of an iconic adaptive radiation. *bioRxiv*, pp.2024-07.
320

321 Gabriel, L., Brůna, T., Hoff, K. J., Ebel, M., Lomsadze, A., Borodovsky, M., & Stanke, M.
322 2024. BRAKER3: Fully automated genome annotation using RNA-seq and protein evidence
323 with GeneMark-ETP, AUGUSTUS, and TSEBRA. *Genome Research*.
324 <https://doi.org/10.1101/gr.278090.123>
325

326 Gotoh, O. 2008. A space-efficient and accurate method for mapping and aligning cDNA
327 sequences onto genomic sequence. *Nucleic Acids Res.* 36(8), 2630-2638.
328

329 Godwin, J. and Fautin, D.G., 1992. Defense of host actinians by anemonefishes. *Copeia*.
330 1992(3) pp.902-908
331

332 Guan D, et al. 2020. Identifying and removing haplotypic duplication in primary genome
333 assemblies. *Bioinformatics* 36:2896–2898. doi: [10.1093/bioinformatics/btaa025](https://doi.org/10.1093/bioinformatics/btaa025).
334

335 Hoff KJ, Lange S, Lomsadze A, Borodovsky M, Stanke M. 2016. BRAKER1: unsupervised
336 RNA-Seq-based genome annotation with GeneMark-ET and AUGUSTUS. *Bioinformatics*
337 32(5), 767-769.
338

339 Hoff KJ, Lomsadze A, Borodovsky M, Stanke M. 2019. Whole-genome annotation with
340 BRAKER. *Methods Mol Biol.* 1962:65-95.
341

342 Holbrook, S.J. and Schmitt, R.J., 2005. Growth, reproduction and survival of a tropical sea
343 anemone (Actiniaria): benefits of hosting anemonefish. *Coral Reefs*, 24, pp.67-73.
344

345 Huang, N., & Li, H. 2023. compleasm: a faster and more accurate reimplementation of
346 BUSCO. *Bioinformatics* 39(10):btad595.
347

348 Iwata H, Gotoh O. 2012. Benchmarking spliced alignment programs including Spaln2, an
349 extended version of Spaln that incorporates additional species-specific features. *Nucleic Acids*
350 *Res.* 40(20), e161-e161.

351

352 Johansen, S. D., Chi, S. I., Dubin, A., & Jørgensen, T. E. 2021. The Mitochondrial Genome of
353 the Sea Anemone *Stichodactyla haddoni* Reveals Catalytic Introns, Insertion-Like Element,
354 and Unexpected Phylogeny. *Life (Basel, Switzerland)*, 11(5), 402.
355 <https://doi.org/10.3390/life11050402>

356

357 Kim D, Paggi JM, Park C, Bennett C, Salzberg SL. 2019. Graph-based genome alignment and
358 genotyping with HISAT2 and HISAT-genotype. *Nat Biotechnol.* 37(8):907-915.

359

360 Kovaka S, et al. 2019. Transcriptome assembly from long-read RNA-seq alignments with
361 StringTie2. *Genome Biology*. 20(1):1-13.

362

363 Kuznetsov D, et al. 2023. OrthoDB v11: annotation of orthologs in the widest sampling of
364 organismal diversity. *Nucleic Acids Research*. 51(D1), pp.D445-D451.

365

366 Laetsch DR, Blaxter ML. 2017. BlobTools: Interrogation of genome assemblies. *F1000*
367 *Research*. 6:1287. doi: [10.12688/f1000research.12232.1](https://doi.org/10.12688/f1000research.12232.1).

368

369 Li, H. 2023. Protein-to-genome alignment with miniprot. *Bioinformatics*, 39(1), btad014.
370 <https://doi.org/10.1093/bioinformatics/btad014>

371

372 Litsios, G., Sims, C.A., Wüest, R.O., Pearman, P.B., Zimmermann, N.E. and Salamin, N.,
373 2012. Mutualism with sea anemones triggered the adaptive radiation of clownfishes. *BMC*
374 *Evolutionary Biology*, 12, pp.1-15.

375

376 Lubbock, R., 1981. The clownfish/anemone symbiosis: a problem of cellular
377 recognition. *Parasitology*, 82(1), pp.159-173.

378

379 Manni M, Berkeley MR, Seppey M, Simão FA, Zdobnov EM. 2021. BUSCO Update: Novel
380 and Streamlined Workflows along with Broader and Deeper Phylogenetic Coverage for

381 Scoring of Eukaryotic, Prokaryotic, and Viral Genomes. *Molecular Biology & Evolution*.
382 38:4647–4654. doi: [10.1093/molbev/msab199](https://doi.org/10.1093/molbev/msab199).

383

384 Marçais, G., & Kingsford, C. 2011. A fast, lock-free approach for efficient parallel counting
385 of occurrences of k-mers. *Bioinformatics*, 27(6), 764–770.
386 <https://doi.org/10.1093/bioinformatics/btr011>

387

388 Marcionetti, A. and Salamin, N., 2023. Insights into the genomics of clownfish adaptive
389 radiation: the genomic substrate of the diversification. *Genome Biology and Evolution*, 15(7),
390 p.evad088.

391

392 Marcionetti, A., Rossier, V., Roux, N., Salis, P., Laudet, V. and Salamin, N., 2019. Insights
393 into the genomics of clownfish adaptive radiation: genetic basis of the mutualism with sea
394 anemones. *Genome Biology and Evolution*, 11(3), pp.869-882.

395

396 Nevers, Y., Rossier, V., Train, C. M., Altenhoff, A., Dessimoz, C., & Glover, N. 2022.
397 *Multifaceted quality assessment of gene repertoire annotation with OMArk* (p.
398 2022.11.25.517970). *bioRxiv*. <https://doi.org/10.1101/2022.11.25.517970>

399

400 Pertea, G., & Pertea, M. 2020. GFF utilities: GffRead and GffCompare. *F1000Research*, 9.
401

402 Ranallo-Benavidez, T. R., Jaron, K. S., & Schatz, M. C. 2020. GenomeScope 2.0 and
403 Smudgeplot for reference-free profiling of polyploid genomes. *Nature Communications*,
404 11(1), 1432. <https://doi.org/10.1038/s41467-020-14998-3>

405

406 Rhie A, Walenz BP, Koren S, Phillippy AM. 2020. Merqury: reference-free quality,
407 completeness, and phasing assessment for genome assemblies. *Genome Biol*. 21:245. doi:
408 [10.1186/s13059-020-02134-9](https://doi.org/10.1186/s13059-020-02134-9).

409

410 Roopin, M., Henry, R.P. and Chadwick, N.E., 2008. Nutrient transfer in a marine mutualism:
411 patterns of ammonia excretion by anemonefish and uptake by giant sea anemones. *Marine
412 Biology*, 154, pp.547-556.

413

414 Roopin, M. and Chadwick, N.E., 2009. Benefits to host sea anemones from ammonia
415 contributions of resident anemonefish. *Journal of Experimental Marine Biology and*
416 *Ecology*, 370(1-2), pp.27-34.
417

418 Szczebak, J.T., Henry, R.P., Al-Horani, F.A. and Chadwick, N.E., 2013. Anemonefish
419 oxygenate their anemone hosts at night. *Journal of Experimental Biology*, 216(6), pp.970-976.
420

421 Simão, F. A., Waterhouse, R. M., Ioannidis, P., Kriventseva, E. V., & Zdobnov, E. M. 2015.
422 BUSCO: Assessing genome assembly and annotation completeness with single-copy
423 orthologs. *Bioinformatics*, 31(19), 3210–3212. <https://doi.org/10.1093/bioinformatics/btv351>
424

425 Smit, AFA and Green, P RepeatMasker at <http://www.repeatmasker.org>
426

427 SRA Toolkit Development Team. 2020. SRA Toolkit.
428 <https://trace.ncbi.nlm.nih.gov/Traces/sra/sra.cgi?view=software>.
429

430 Stanke M, Diekhans M, Baertsch R, Haussler, D. 2008. Using native and syntenically mapped
431 cDNA alignments to improve de novo gene finding. *Bioinformatics*, 24(5), 637-644.
432

433 Stanke, M., Schöffmann, O., Morgenstern, B., Waack, S. 2006. Gene prediction in eukaryotes
434 with a generalized hidden Markov model that uses hints from external sources. *BMC*
435 *Bioinformatics*, 7(1), 62.
436

437 Tillich, M., Lehwark, P., Pellizzer, T., Ulbricht-Jones, E. S., Fischer, A., Bock, R., & Greiner,
438 S. 2017. GeSeq – versatile and accurate annotation of organelle genomes. *Nucleic Acids*
439 *Research*, 45(W1), W6–W11. <https://doi.org/10.1093/nar/gkx391>
440

441 Titus, B.M., Benedict, C., Laroche, R., Gusmão, L.C., Van Deusen, V., Chiodo, T., Meyer,
442 C.P., Berumen, M.L., Bartholomew, A., Yanagi, K. and Reimer, J.D., 2019. Phylogenetic
443 relationships among the clownfish-hosting sea anemones. *Molecular Phylogenetics and*
444 *Evolution*, 139, p.106526.
445

446 Titus, B.M., Bennett-Smith, M.F., Chiodo, T. and Rodríguez, E., 2024. The clownfish-hosting
447 sea anemones (Anthozoa: Actiniaria): updated nomenclature, biogeography, and practical
448 field guide. *Zootaxa*, 5506(1), pp.1-34.
449

450 Verde, E.A., Cleveland, A. and Lee, R.W., 2015. Nutritional exchange in a tropical tripartite
451 symbiosis II: direct evidence for the transfer of nutrients from host anemone and
452 zooxanthellae to anemonefish. *Marine Biology*, 162, pp.2409-2429.
453

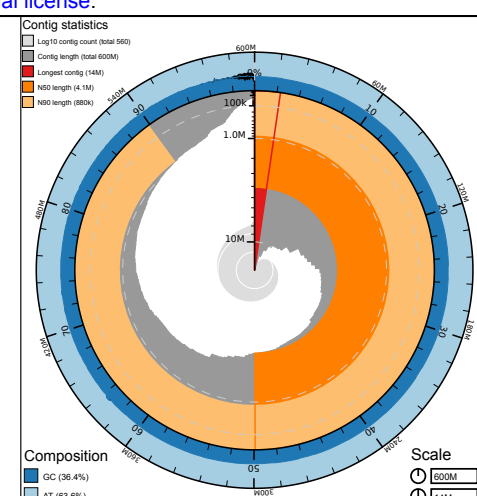
454 Vulture GW, et al. 2017. GenomeScope: fast reference-free genome profiling from short
455 reads. *Bioinformatics*. 33:2202–2204. doi: 10.1093/bioinformatics/btx153.

456 **Figures**

457

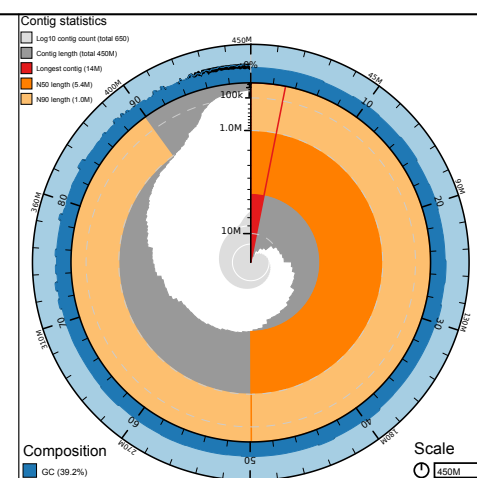
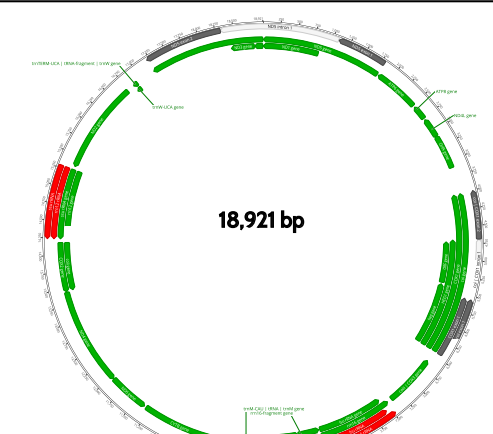
458 Figure 1. Long-read mitochondrial and nuclear genome assemblies for the clownfish hosting
459 sea anemone species A) *Entacmaea quadricolor*, B) *Stichodactyla haddoni*, and C)
460 *Radianthus doreensis*. Pictures of each species are the individuals sequenced in this study.
461 Circularized and annotated mitogenomes were visualized with Geneious version 2024.0.
462 BlobToolKit snailplots representing nuclear genome assembly statistics including genome
463 size, largest scaffold length, N50 and N90 lengths, and GC composition. Snailplots are
464 divided into 1,000 size-ordered bins around the circumference with each bin representing
465 0.1% of the assembly length. The distribution of contig lengths is shown in dark gray with the
466 plot radius scaled to the longest contig present in the assembly (the smallest of the three arcs,
467 also shown in red). Next two sectors in size (orange and pale-orange arcs) show the N50 and
468 N90 contig lengths, respectively. The pale gray spiral shows the cumulative scaffold count on
469 a log scale with white scale lines showing successive orders of magnitude. The dark-blue and
470 pale-blue area around the outside of the plot shows the distribution of GC, AT, and N
471 percentages in the same bins as the inner plot.

A



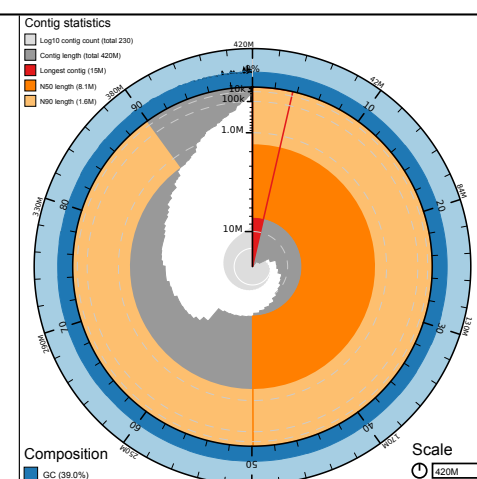
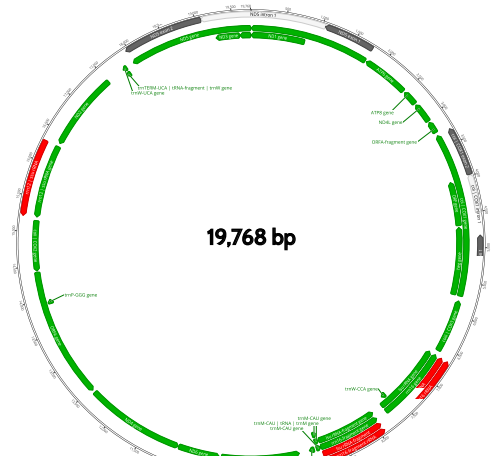
B

Stichodactyla haddoni



C

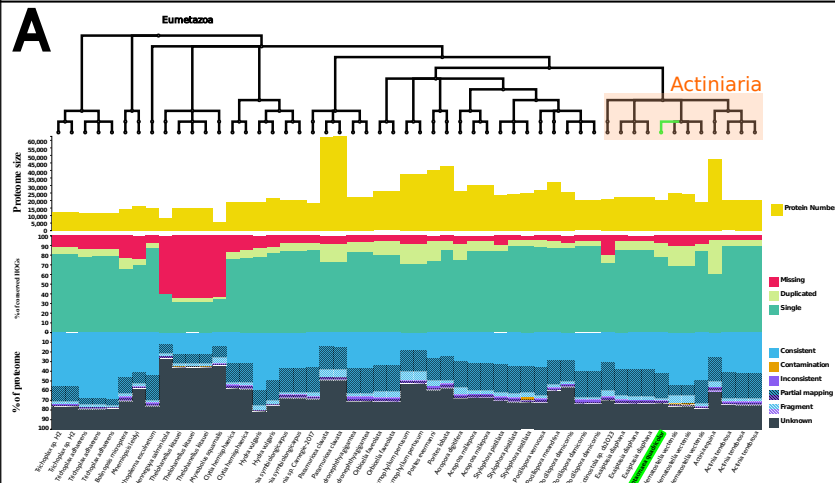
Radianthus doreensis



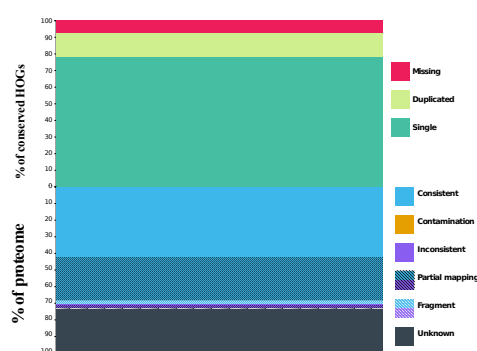
472 Figure 2. OMArk quality assessment of genome annotations. A, C, &E) OMArk comparison
473 plots showing genome annotation statistics for *Entacmaea quadricolor*, *Stichodactyla*.
474 *haddoni* and *Radianthus doreensis* in reference to other members of Eumetazoa. Positions of
475 the clownfish-hosting sea anemones sequenced in this study are highlighted in green. List of
476 available proteome accessions used for the comparisons in Supplementary material. B, D, &
477 F) detailed proteome assessment for each species of clownfish-hosting sea anemones
478 sequenced in this study.

Entacmaea quadricolor

A

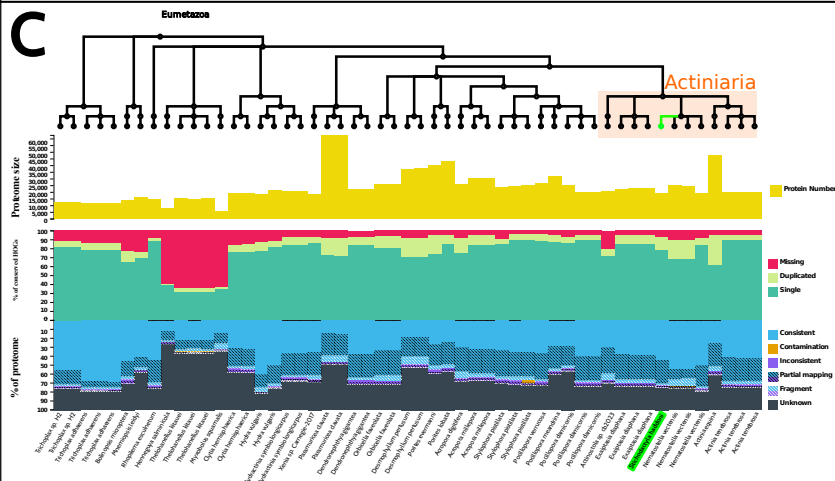


B

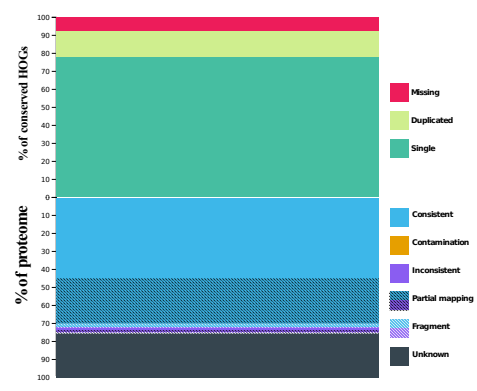


Stichodactyla haddoni

C

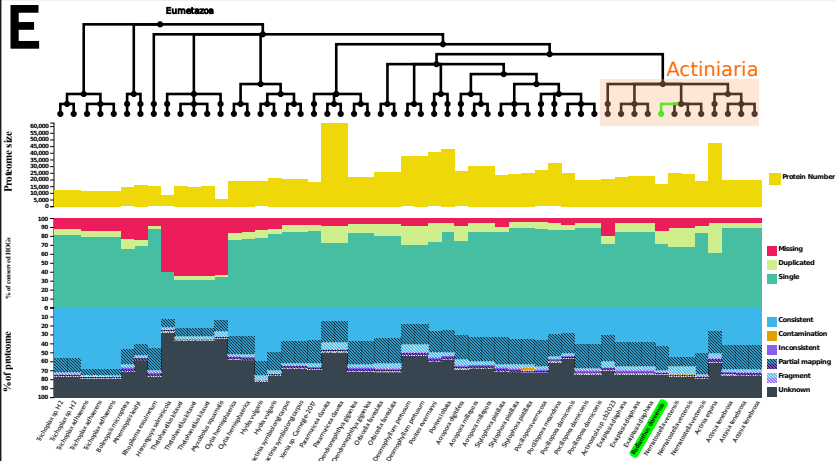


D



Radianthus doreensis

E



F

